



**Mutations in FUS, an RNA Processing Protein,  
Cause Familial Amyotrophic Lateral Sclerosis Type  
6**

Caroline Vance, *et al.*  
*Science* **323**, 1208 (2009);  
DOI: 10.1126/science.1165942

***The following resources related to this article are available online at  
www.sciencemag.org (this information is current as of March 9, 2009 ):***

**Updated information and services**, including high-resolution figures, can be found in the online version of this article at:

<http://www.sciencemag.org/cgi/content/full/323/5918/1208>

**Supporting Online Material** can be found at:

<http://www.sciencemag.org/cgi/content/full/323/5918/1208/DC1>

A list of selected additional articles on the Science Web sites **related to this article** can be found at:

<http://www.sciencemag.org/cgi/content/full/323/5918/1208#related-content>

This article **cites 27 articles**, 11 of which can be accessed for free:

<http://www.sciencemag.org/cgi/content/full/323/5918/1208#otherarticles>

This article appears in the following **subject collections**:

Genetics

<http://www.sciencemag.org/cgi/collection/genetics>

Information about obtaining **reprints** of this article or about obtaining **permission to reproduce this article** in whole or in part can be found at:

<http://www.sciencemag.org/about/permissions.dtl>

mutant. Subcellular localization of FUS/TLS was additionally studied by compartmental fractionation of SKNAS cells transfected with WT, R521G, or H517Q FUS/TLS–GFP fusion proteins. Immunoblotting of fractions followed by immunostaining with an antibody to GFP demonstrated a substantially higher ratio of soluble cytosolic to soluble nuclear FUS/TLS for both mutants (Fig. 3B). Additionally, a higher ratio of total insoluble to soluble nuclear FUS/TLS protein was also seen for both mutants, although it is more pronounced for the R521G mutant; this reflected both an increase in total insoluble FUS and a decrease in soluble nuclear FUS (fig S3).

The major defined RNA-interacting domains of FUS/TLS are located in the mid-region of the protein, from amino acids 280 to 370, encoded by exons 9 to 11 (10, 11); sequences of target RNA domains recognized by FUS/TLS have been reported. To show that the FALS-associated FUS/TLS mutations detected here do not alter the RNA-binding domain of FUS, we performed *in vitro* RNA-binding experiments with recombinant histidine (His)-tagged mutant and WT FUS/TLS proteins and RNA 24-nucleotide oligomer containing GGUG motifs and known to bind FUS/TLS (10). Binding of the RNA oligomers was similar for mutant and WT FUS/TLS protein (fig. S4).

FUS/TLS is a nucleoprotein that functions in DNA and RNA metabolism (12–15). It has also been implicated in tumorigenesis (6, 16, 17) and RNA metabolism. FUS/TLS knockout mice show perinatal mortality (18) or male sterility and radiation sensitivity (19). FUS/TLS-deficient neurons show decreased spine arborization with abnormal morphology. In hippocampal neuronal slice cultures, the protein is found in RNA granules that are transported to dendritic spines for local RNA translation in response to metabotropic glutamate receptor (mGluR5) stimulation (20).

We detected 13 FUS/TLS mutations in patients with FALS but none in patients with SALS. We estimate that FUS/TLS mutations are detected in about 5% of FALS; this is comparable to the frequency of TDP43 gene mutations in ALS but less than that for SOD1 (mutated in ~20% of FALS cases). The FUS/TLS mutations described here led to cytoplasmic retention and apparent aggregation of FUS/TLS. This is reminiscent of several models of the pathogenesis of FALS that are mediated by the aggregation of mutant superoxide dismutase (21) and the mislocalization in ALS of both mutant and WT TDP43 (4, 22). FUS/TLS has also been reported to be a major nuclear aggregate-interacting protein in a model of Huntington's disease (23). Genes implicated in other motor neuron diseases also involve aspects of DNA and RNA metabolism [table S5 in (24)]; understanding the convergent pathophysiology of these genetic variants will provide insights into new targets for therapies for the motor neuron diseases.

#### References and Notes

1. L. M. Nelson, *Clin. Neurosci.* **3**, 327 (1995).
2. D. R. Rosen, *Nature* **364**, 362 (1993).
3. E. Kabashi *et al.*, *Nat. Genet.* **40**, 572 (2008).

4. J. Sreedharan *et al.*, *Science* **319**, 1668 (2008).
5. V. M. Van Deerlin *et al.*, *Lancet Neurol.* **7**, 409 (2008).
6. A. Crozat, P. Aman, N. Mandahl, D. Ron, *Nature* **363**, 640 (1993).
7. In the mutants, other amino acids were substituted at certain locations; for example, R182Q indicates that arginine at position 182 was replaced by glutamine. Single-letter abbreviations for the amino acid residues are as follows: A, Ala; C, Cys; D, Asp; E, Glu; F, Phe; G, Gly; H, His; I, Ile; K, Lys; L, Leu; M, Met; N, Asn; P, Pro; Q, Gln; R, Arg; S, Ser; T, Thr; V, Val; W, Trp; and Y, Tyr.
8. P. Sapp *et al.*, *Am. J. Hum. Genet.* **73**, 397 (2003).
9. Materials and methods are available as supporting material on Science Online.
10. A. Lerga *et al.*, *J. Biol. Chem.* **276**, 6807 (2001).
11. F. Morohoshi *et al.*, *Gene* **221**, 191 (1998).
12. H. Baechtold *et al.*, *J. Biol. Chem.* **274**, 34337 (1999).
13. P. Bertrand, A. T. Akhmedov, F. Delacote, A. Durrbach, B. S. Lopez, *Oncogene* **18**, 4515 (1999).
14. L. Yang, L. J. Embree, S. Tsai, D. D. Hickstein, *J. Biol. Chem.* **273**, 27761 (1998).
15. X. Wang *et al.*, *Nature* **454**, 126 (2008).
16. T. H. Rabbitts, A. Forster, R. Larson, P. Nathan, *Nat. Genet.* **4**, 175 (1993).
17. W. J. Law, K. L. Cann, G. G. Hicks, *Brief. Funct. Genomics Proteomics* **5**, 8 (2006).
18. G. G. Hicks *et al.*, *Nat. Genet.* **24**, 175 (2000).
19. M. Kuroda *et al.*, *EMBO J.* **19**, 453 (2000).
20. R. Fujii *et al.*, *Curr. Biol.* **15**, 587 (2005).
21. S. Boillee, C. Vande Velde, D. W. Cleveland, *Neuron* **52**, 39 (2006).
22. M. J. Winton *et al.*, *J. Biol. Chem.* **283**, 13302 (2008).
23. H. Doi *et al.*, *J. Biol. Chem.* **283**, 6489 (2008).
24. C. Simpson *et al.*, *Hum. Mol. Genet.* **18** (no. 3), 472 (2008).

25. We gratefully acknowledge I. Carr (University of Leeds, UK) for support with AutoSNPa and IBDfinder software, A. Storey for assistance with sequencing, C. LeClerc for genealogical investigations, and D. Crowe for administrative assistance. This work was supported by NIH grants NS050557 (R.H.B. and T.K.) and NS050641 (T.S., R.H.B., J.L.H., and M.P.-V.). R.H.B. also receives support from the Angel Fund, the ALS Therapy Alliance, the ALS Association Project ALS, the Al-Athel ALS Research Foundation, and the Pierre L. de Bourgknecht ALS Research Foundation. T.S. also receives support from The Les Turner ALS Foundation, Vena E. Schaff ALS Research Fund, Harold Post Research Professorship, Herbert and Florence C. Wenske Foundation, Ralph and Marian Falk Medical Research Trust, The David C. Asselin M.D. Memorial Fund, Les Turner ALS Foundation/Herbert C. Wenske Foundation Professorship, Help America Foundation and the ALS Therapy Alliance, Inc. H.R.H. is an investigator of and was supported by the Howard Hughes Medical Institute. R.H.B. is a cofounder of AvitX Inc., which targets development of ALS therapies. R.H.B. and T.J.K. have applied for a patent covering FUS mutations in ALS. We dedicate this report to the memories of Jimmy and Christopher Kennedy, Sharon Timlin, and Ginny Delvecchio.

#### Supporting Online Material

www.sciencemag.org/cgi/content/full/323/5918/1205/DC1  
Materials and Methods

Figs. S1 to S4

Table S1

References

17 September 2008; accepted 6 January 2009  
10.1126/science.1166066

## Mutations in FUS, an RNA Processing Protein, Cause Familial Amyotrophic Lateral Sclerosis Type 6

Caroline Vance,<sup>1\*</sup> Boris Rogelj,<sup>1\*</sup> Tibor Hortobágyi,<sup>1\*</sup> Kurt J. De Vos,<sup>2\*</sup> Agnes Lumi Nishimura,<sup>1</sup> Jemeen Sreedharan,<sup>1</sup> Xun Hu,<sup>1</sup> Bradley Smith,<sup>1</sup> Deborah Ruddy,<sup>1</sup> Paul Wright,<sup>1</sup> Jeban Ganesalingam,<sup>1</sup> Kelly L. Williams,<sup>3</sup> Vineeta Tripathi,<sup>1</sup> Safa Al-Saraj,<sup>1</sup> Ammar Al-Chalabi,<sup>1</sup> P. Nigel Leigh,<sup>1</sup> Ian P. Blair,<sup>3,5</sup> Garth Nicholson,<sup>3,4,5</sup> Jackie de Belleruche,<sup>6</sup> Jean-Marc Gallo,<sup>1</sup> Christopher C. Miller,<sup>1,2</sup> Christopher E. Shaw<sup>1†</sup>

Amyotrophic lateral sclerosis (ALS) is a fatal neurodegenerative disease that is familial in 10% of cases. We have identified a missense mutation in the gene encoding fused in sarcoma (FUS) in a British kindred, linked to ALS6. In a survey of 197 familial ALS index cases, we identified two further missense mutations in eight families. Postmortem analysis of three cases with FUS mutations showed FUS-immunoreactive cytoplasmic inclusions and predominantly lower motor neuron degeneration. Cellular expression studies revealed aberrant localization of mutant FUS protein. FUS is involved in the regulation of transcription and RNA splicing and transport, and it has functional homology to another ALS gene, TARDBP, which suggests that a common mechanism may underlie motor neuron degeneration.

Amyotrophic lateral sclerosis (ALS) causes progressive muscular weakness due to the degeneration of motor neurons in the brain and spinal cord. The average age at onset is 60 years, and annual incidence is 1 to 2 per 100,000. Death due to respiratory failure occurs on average 3 years after symptom onset (1). Autosomal dominant familial ALS (FALS) is clinically and pathologically indistinguishable from sporadic disease (SALS) and accounts for ~10%

of cases (2). Three genes have been confidently linked to classical FALS: SOD1, encoding CuZn superoxide dismutase (SOD1) (ALSI OMIM 105400) (3); ANG, encoding angiogenin (4–6); and TARDBP, encoding TAR DNA binding protein TDP-43 (ALSI OMIM 612069) (7). SOD1 mutations are detected in 20% of FALS and 5% of SALS cases (3, 8). Mice transgenic for mutant human SOD1 develop selective motor neuron degeneration due to a toxic gain of function (9) that is not cell autonomous

(10) and is associated with multimeric detergent-resistant cytoplasmic mutant SOD1 aggregates (11). Ubiquitinated TDP-43 inclusions are detected in the perikaryon in the motor neurons of ~90% of ALS cases and in the cortical neurons of a subset of frontotemporal lobar dementia (FTLD) cases (12, 13). Fourteen missense TDP-43 mutations have now been associated with ALS, and all but one reside in the C-terminal domain (7, 14–16).

In addition, individual FALS kindreds have been linked to chromosomes 18q (*ALS3*, OMIM 606640) (17) and 20p (*ALS7*, OMIM 608031) (18), whereas multiple kindreds with ALS and FTLD have been linked to chromosomes 9q (FTD/ALS1 OMIM 105550) (19) and 9p (*ALSFTD2*, OMIM 611454) (20–22). We previously linked one large multigenerational British kindred (F1) to a 42-Mb region on chromosome 16 with a multipoint lod score (logarithm of the odds ratio for linkage) of 3.85 (*ALS6* OMIM 608030) (23). As two more individuals developed ALS, we repeated the genome-wide scan using the 10K single-nucleotide polymorphism (SNP) arrays. This confirmed linkage to chromosome 16 with a conserved haplotype containing more than 400 genes (fig. S1). Using a candidate gene approach, we sequenced 279 exons from 32 genes and expressed sequence tags (ESTs) and 10 noncoding RNAs (tables S1 and S2). After our detection of mutations in *TARDBP*, we prioritized six genes containing similar domains within the linked region. A single base-pair change was identified in exon 15 of *FUS* (also known as translocation in liposarcoma or *TLS*) in the proband from the F1 kindred (fig. S2A). This change is predicted to result in an arginine to cysteine substitution at position 521 (R521C), which is in a highly conserved region at the very C terminus of the protein (fig. S2, B and C). The 1561 C>T (R521C) mutation was present in the DNA of all six affected members of F1 and cosegregated with the linked haplotype (Fig. 1A).

To determine the frequency of *FUS* mutations in FALS, we screened 197 index FALS cases in which *SOD1*, *VAPB*, *ANG*, *Dynactin*, *CHMP2B*, and *TARDBP* mutations had been excluded. We identified the same R521C mutation in a further four families, including three affected individuals from one kindred (ALS53) (Fig. 1B) and three

more index FALS cases. In addition, we found a different base-pair change that is predicted to result in an arginine to histidine substitution, also at position 521 (1562 G>A, R521H) (fig. S2, A to C). The R521H mutation was identified in two families where it segregates with disease (F1015 and ALS156) (Fig. 1, C and D) and one index case. A third mutation was identified in exon 14

that is predicted to result in an arginine to glycine substitution at position 514 (1540 A>G, R514G) (fig. S2, A to C). This was detected in two affected members of the pedigree F1083 (Fig. 1E). No mutations were detected in exons 1 to 13 in the other FALS cases. Exons 14 and 15 of *FUS* were sequenced in 400 age, sex, and ethnically matched controls, and no mutations were detected.

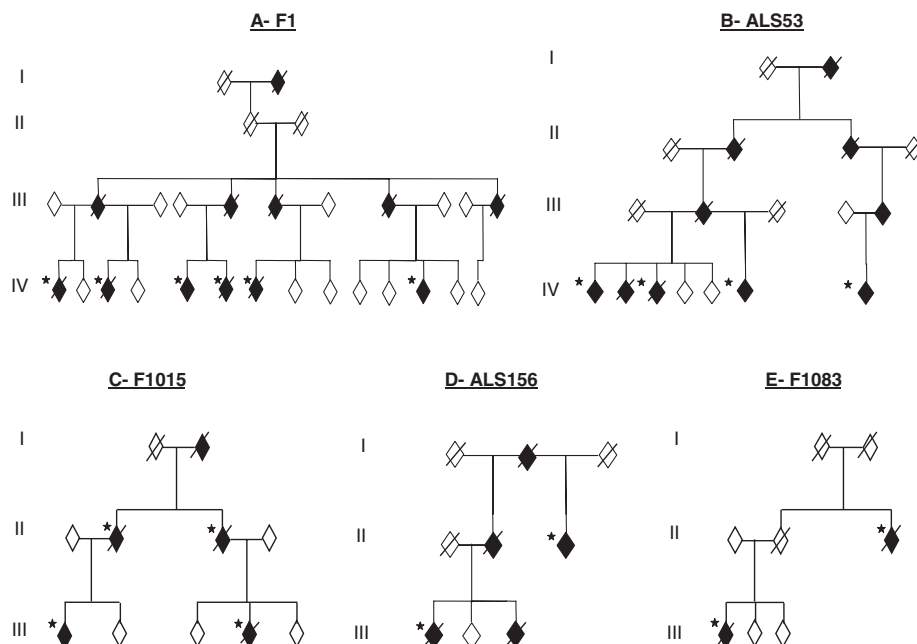


**Fig. 1.** *FUS* mutations segregate with disease in five dominant ALS kindreds. Affected individuals are indicated by black symbols and unaffected individuals by open symbols. Slashed symbols indicate deceased individuals. Asterisks indicates an affected individual for whom DNA was available. All affected individuals tested carried their families' mutation. Gender, birth order, and the mutation status of unaffected individuals have been omitted for reasons of confidentiality.

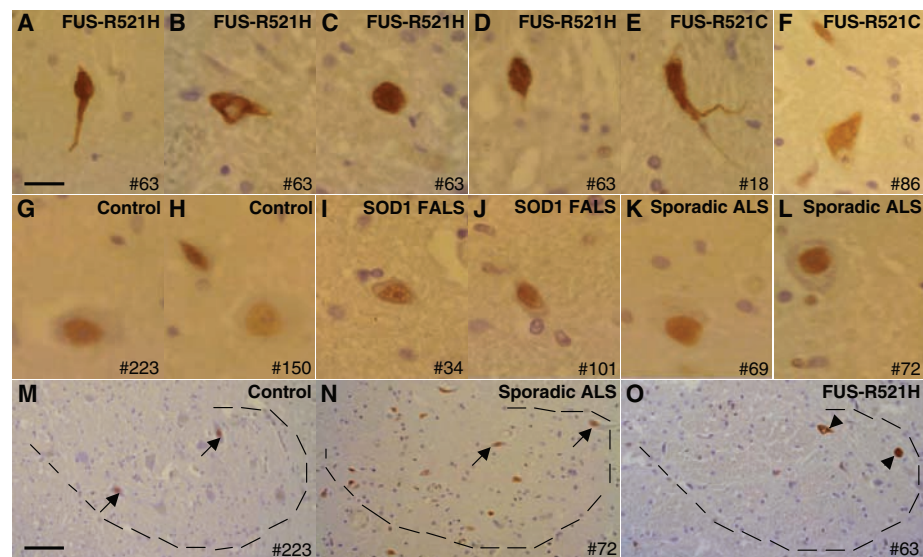


**Fig. 2.** Patients with *FUS* mutations develop cytoplasmic *FUS* immunoreactive inclusions in lower motor neurons. Antibody to *FUS* immunolabels inclusions within the anterior horn (dotted line) of the spinal cord in patients with *FUS* mutations (A to F and arrowheads in O). Staining in controls (G, H, and M), mutant *SOD1* FALS (I and J), and SALS (K, L, and N) demonstrate diffuse nuclear staining (arrows) with variable intensity without inclusions. Scale bars, 12  $\mu$ m [(A) to (L)], 50  $\mu$ m [(M) to (O)].

<sup>1</sup>Department of Clinical Neuroscience, King's College London, Medical Research Council (MRC) Centre for Neurodegeneration Research, Institute of Psychiatry, London SE5 8AF, UK.

<sup>2</sup>Department of Neuroscience, King's College London, MRC Centre for Neurodegeneration Research, Institute of Psychiatry, London SE5 8AF, UK. <sup>3</sup>Northcott Neuroscience Laboratory, Australian and New Zealand Army Corps (ANZAC) Research Institute, Concord, NSW 2139, Australia. <sup>4</sup>Molecular Medicine Laboratory, Concord Hospital, Concord, NSW 2139, Australia.

<sup>5</sup>Faculty of Medicine, University of Sydney, Sydney, NSW 2139, Australia. <sup>6</sup>Division of Neurosciences and Mental Health, Faculty of Medicine, Imperial College London, Hammersmith Hospital, London W12 0NN, UK.

\*These authors contributed equally to this work.

†To whom correspondence should be addressed. E-mail: chris.shaw@iop.kcl.ac.uk

The frequency of FUS mutations in British and Australian SOD1-negative cases is ~4% (equivalent to 3% of all FALS cases).

Sufficient information to define a clinical phenotype was available in 20 individuals with FUS mutations. There was an even gender distribution (9 male, 11 female), the average age at onset was 44.5 years ( $n = 20$ ), and average survival was 33 months ( $n = 18$ ). The site of onset was cervical (10), lumbar (5), and bulbar (3). No affected individual developed cognitive deficits. Three cases with the FUS<sub>R521C</sub> and FUS<sub>R521H</sub> mutations underwent detailed neuropathological examination. All revealed severe lower motor neuron loss in the spinal cord (Fig. 2O) and to a lesser degree in the brain stem, whereas dorsal horn neurons appeared unaffected. There was evidence of mild myelin loss in the dorsal columns, but only one case had major pallor of the corticospinal tracts.

There was mild to moderate upper motor neuron loss in the motor cortex. Ubiquitin and p62-immunopositive skeinlike cytoplasmic inclusions in anterior horn motor neurons of the spinal cord, which are hallmarks of classical ALS, were very rare, and TDP-43-positive inclusions within the cytoplasm and nucleus of neurons and glial cells were absent. Antibody to FUS labeled large globular and elongated cytoplasmic inclusions in spinal cord motor neurons and dystrophic neurites in all three ALS cases with FUS mutations (Fig. 2, A to F, and O). These were absent in normal control individuals (Fig. 2, G, H, and M), SOD1 mutant ALS cases (Fig. 2, I and J), and sporadic ALS cases (Fig. 2, K, L, and N).

To assess the functional importance of these mutations, we transiently expressed N-terminally hemagglutinin (HA)-tagged wild-type FUS (FUS<sub>WT</sub>) and two mutants, (FUS<sub>R521C</sub> and FUS<sub>R521H</sub>) in

CV-1 and N2A cell lines and rat cortical neurons. Staining for endogenous FUS in nontransfected cells indicated that the protein is predominantly localized to the nucleus. Transfected cells show an increase in cytoplasmic localization of the FUS<sub>R521C</sub> and FUS<sub>R521H</sub> protein when compared to the wild type, both with immunofluorescent labeling and by immunoblot (Fig. 3).

FUS is a ubiquitously expressed, predominantly nuclear, protein that is involved in DNA repair and the regulation of transcription, RNA splicing, and export to the cytoplasm. The N terminus has a transcriptional activation domain which, after chromosomal translocation, produces fusion proteins that can cause Ewing's sarcoma and acute myeloid leukemia (24). The C terminus contains RNA recognition motif (RRM), Arg-Gly-Gly (RGG) repeat rich, and zinc finger domains involved in RNA processing. FUS binds to the motor proteins kinesin (KIF5) (25) and myosin-Va (26) and is involved in mRNA transport; it is notable that defects in axonal transport are a pathological feature of ALS (27).

Mutations in the C-terminal domain of TDP-43 have been linked to ALS (7, 14–16) and are associated with mislocalization and inclusion formation, providing an almost exact parallel with FUS mutations. In the case of TDP-43 proteinopathies, it is not clear whether disease is due to a toxic gain, or loss, of function. Although toxicity might be a consequence of misfolded proteins overwhelming the protein surveillance machinery, the loss of TDP-43 from the nucleus in neurons with inclusions provides circumstantial evidence that nuclear RNA processing may be impaired. Equally, the presence of cytoplasmic aggregates might lead to the sequestration of proteins and/or RNAs in the cytoplasm, causing selective toxicity to cortical and motor neurons. The absence of TDP-43 inclusions in mutant FUS ALS cases implies that the FUS disease pathway is independent of TDP-43 aggregation. An exploration of how these two functionally related proteins cause neurodegeneration should provide new insights into the mechanisms underlying ALS pathogenesis.

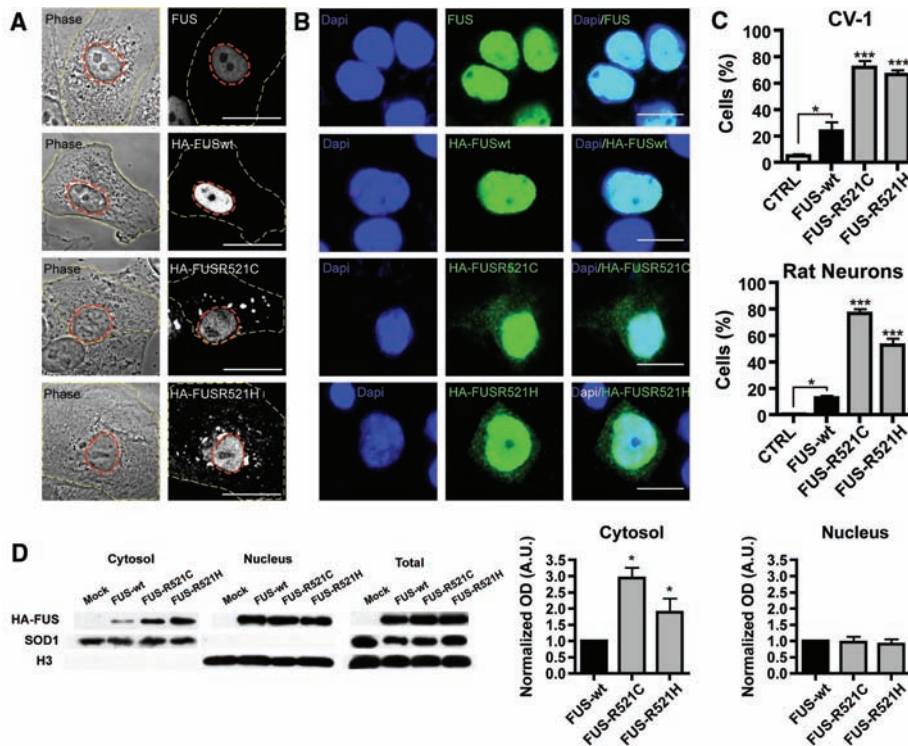


**Fig. 3.** FUS mutations cause subcellular mislocalization. (A and B) The subcellular localization of endogenous FUS, transfected wild-type (HA-FUS<sub>WT</sub>), and FUS mutants (HA-FUS<sub>R521C</sub>, HA-FUS<sub>R521H</sub>) was determined in CV-1 cells (A) and rat cortical neurons (B) by immunofluorescence. The plasma membrane (A, yellow dash) and nucleus (A, red dash) of representative CV-1 cells are outlined on phase contrast (A, left panel) and corresponding FUS immunofluorescence images (A, right panel). Nuclear diamidino-2-phenylindole (DAPI) staining (B, left panel), FUS immunofluorescence (B, middle panel), and overlay (B, right panel) of representative cortical neurons are shown. Scale bars, 25  $\mu$ m (A), 10  $\mu$ m (B). (C) The percentage of CV-1 cells (upper panel) and cortical neurons (lower panel) showing FUS staining in the cytoplasm was significantly increased for mutant forms of FUS compared to wild-type and endogenous. Statistical significance was determined by one-way analysis of variance ( $P < 0.0001$  for CV1 and neurons) followed by Bonferroni's Multiple Comparison Test (\*,  $P < 0.05$ ; \*\*\*,  $P < 0.001$ ). (D) FUS mutants show a significant increase in the cytosolic fraction. N2A cells transfected with FUS<sub>WT</sub>, FUS<sub>R521C</sub>, and FUS<sub>R521H</sub> were separated into cytosolic and nuclear fractions, and the amount of transfected FUS was determined by densitometry of antibody to HA immunoblots (mean  $\pm$  SEM,  $n = 3$ ). The purity of fractions was determined with antibody to SOD1 (cytosol) and antibody to histone H3 (nucleus), and the transfection efficiencies were compared in total cell lysates. Statistical significance was determined by Wilcoxon Signed Rank Test (\*,  $P < 0.05$ ).

**References and Notes**

- C. E. Shaw, A. al-Chalabi, N. Leigh, *Curr. Neurol. Neurosci. Rep.* **1**, 69 (2001).
- C. E. Shaw *et al.*, *Neurology* **49**, 1612 (1997).
- D. R. Rosen, *Nature* **364**, 362 (1993).
- F. L. Conforti *et al.*, *Neuromuscul. Disord.* **18**, 68 (2008).
- M. J. Greenway *et al.*, *Nat. Genet.* **38**, 411 (2006).
- A. Paubel *et al.*, *Arch. Neurol.* **65**, 1333 (2008).
- J. Sreedharan *et al.*, *Science* **319**, 1668 (2008).
- C. E. Shaw *et al.*, *Ann. Neurol.* **43**, 390 (1998).
- M. E. Gurney, H. Pu, A. Y. Chiu, *Science* **264**, 1772 (1994).
- S. Boillee *et al.*, *Science* **312**, 1389 (2006).
- J. Wang, G. Xu, D. R. Borchelt, *Neurobiol. Dis.* **9**, 139 (2002).
- I. R. Mackenzie *et al.*, *Ann. Neurol.* **61**, 427 (2007).
- M. Neumann *et al.*, *Science* **314**, 130 (2006).
- M. A. Gitcho *et al.*, *Ann. Neurol.* **63**, 535 (2008).
- E. Kabashi *et al.*, *Nat. Genet.* **40**, 572 (2008).
- V. M. Van Deerlin *et al.*, *Lancet Neurol.* **7**, 409 (2008).
- C. K. Hand *et al.*, *Am. J. Hum. Genet.* **70**, 251 (2001).
- P. C. Sapp *et al.*, *Am. J. Hum. Genet.* **73**, 397 (2003).
- B. A. Hosler *et al.*, *JAMA* **284**, 1664 (2000).
- M. Morita *et al.*, *Neurology* **66**, 839 (2006).
- P. N. Valdmanis *et al.*, *Arch. Neurol.* **64**, 240 (2007).

22. C. Vance *et al.*, *Brain* **129**, 868 (2006).  
 23. D. M. Ruddy *et al.*, *Am. J. Hum. Genet.* **73**, 390 (2003).  
 24. W. J. Law, K. L. Cann, G. G. Hicks, *Brief. Funct. Genomics Proteomics* **5**, 8 (2006).  
 25. Y. Kanai, N. Dohmae, N. Hirokawa, *Neuron* **43**, 513 (2004).  
 26. A. Yoshimura *et al.*, *Curr. Biol.* **16**, 2345 (2006).  
 27. K. J. De Vos, A. J. Grierson, S. Ackerley, C. C. Miller, *Annu. Rev. Neurosci.* **31**, 151 (2008).  
 28. This publication is dedicated to the patients and families who have contributed to this project and to B. Coote and C. Cecere for blood sample collection. Postmortem tissues were provided by MRC

Neurodegenerative Diseases Brain Bank. This work was supported in the United Kingdom by grants from the American ALS Association, the Middlemass family, Lady Edith Wolfson Trust, Motor Neurone Disease Association UK, The Wellcome Trust, European Union (APOPI consortium, contract LSHM-CT-2003-503330, and NeuroNE Consortium), National Institute for Health Research Biomedical Research Centre for Mental Health, The South London and Maudsley National Health Service Foundation Trust, Medical Research Council UK, a Jack Cigman grant from King's College Hospital Charity, The Heaton-Ellis Trust, and The Psychiatry Research Trust of the Institute of Psychiatry. In Australia the work was

supported by the Australian National Health and Medical Research Council (CDA 511941) and a Peter Stearne grant from the Motor Neuron Disease Research Institute of Australia.

#### Supporting Online Material

www.sciencemag.org/cgi/content/full/323/5918/1208/DC1  
 Materials and Methods  
 Figs. S1 and S2  
 Tables S1 to S4  
 References

15 September 2008; accepted 16 December 2008  
 10.1126/science.1165942

# Synchronous Hyperactivity and Intercellular Calcium Waves in Astrocytes in Alzheimer Mice

Kishore V. Kuchibhotla,<sup>1,2</sup> Carli R. Lattarulo,<sup>1</sup> Bradley T. Hyman,<sup>1</sup> Brian J. Bacskai<sup>1\*</sup>

Although senile plaques focally disrupt neuronal health, the functional response of astrocytes to Alzheimer's disease pathology is unknown. Using multiphoton fluorescence lifetime imaging microscopy *in vivo*, we quantitatively imaged astrocytic calcium homeostasis in a mouse model of Alzheimer's disease. Resting calcium was globally elevated in the astrocytic network, but was independent of proximity to individual plaques. Time-lapse imaging revealed that calcium transients in astrocytes were more frequent, synchronously coordinated across long distances, and uncoupled from neuronal activity. Furthermore, rare intercellular calcium waves were observed, but only in mice with amyloid- $\beta$  plaques, originating near plaques and spreading radially at least 200 micrometers. Thus, although neurotoxicity is observed near amyloid- $\beta$  deposits, there exists a more general astrocyte-based network response to focal pathology.

Growing evidence supports the hypothesis that in Alzheimer's disease (AD), synapses fail and dendritic spines are lost in the amyloid- $\beta$  (A $\beta$ ) plaque microenvironment through a combination of changes in synaptic drive, calcium overload, and the activation of calcium-dependent degenerative processes (1–4). Neurons, however, make up only part of the brain's volume, with astrocytes making up the bulk of the remainder. Astrocytes form a structurally interconnected network that, *in vitro*, exhibit distinct long-distance signaling properties that might be revealed *in vivo* only after pathological trauma. The idea that neural network dysfunction and degeneration also fully mediate the memory loss in AD does not reflect the growing *in vivo* evidence that astrocytes play an important role in cortical circuit function (5–7). In AD, pathological studies of human cases and mouse models have shown that astrocytes surround plaques and might play a critical role in A $\beta$  deposition and clearance (8–10). Given the profound impact of A $\beta$  deposition on nearby neuronal calcium homeostasis and synaptic function, it is reasonable

to hypothesize that astrocyte networks would also be perturbed and might contribute to cortical dysfunction (11). We sought to test whether senile plaque deposition would similarly affect astrocyte calcium homeostasis or dynamic signaling *in vivo* in a mouse model of AD.

To answer these questions, we used multiphoton fluorescent lifetime imaging microscopy (FLIM) to measure resting calcium levels in astrocytes of live mice with cortical plaques (12). We multiplexed the fluorescent properties of a small-molecule calcium dye [Oregon-Green BAPTA-1 (OGB)] in the same experimental model and for the same group of cells (Fig. 1A); we used OGB both as a relative indicator of astrocytic activity (intensity) and as a quantitative measure of steady-state intracellular calcium concentration ([Ca]<sub>i</sub>) (lifetime). We used mice that express mutant human A $\beta$  precursor protein (APP) and mutant presenilin 1 (PS1) (APP<sup>swe</sup>:PS1 $\Delta$ E9) in neurons. These mutations lead to an increase in A $\beta$  production and plaque deposition beginning at ~4.5 months of age (13, 14). In mice with plaques, resting [Ca]<sub>i</sub> in astrocytes was higher than in wild-type animals (Fig. 1, B to F). The resting [Ca]<sub>i</sub> of astrocytes in wild-type mice was  $81 \pm 3$  nM, whereas in transgenic mice the resting [Ca]<sub>i</sub> was  $149 \pm 6$  nM ( $P < 0.05$ ). We confirmed that the surrounding neuropil signal minimally contaminated the astrocyte [Ca]<sub>i</sub> (fig. S2). We next mapped the spatial distribution of astrocytes versus A $\beta$

plaque location in three dimensions (fig. S3). There was no effect of plaque proximity on resting [Ca]<sub>i</sub> in individual astrocytes (Fig. 1G;  $n > 25$  cells per bin). However, plaques deposit rapidly in these mice, so that very few astrocytes were farther than 100  $\mu$ m away from a plaque.

Using time-lapse calcium imaging of OGB intensity, we measured spontaneous astrocytic activity. Astrocytes in adult APP/PS1 mice (6 to 8 months old) with cortical plaques exhibited a significant increase in spontaneous activity (Fig. 2 and movies S1 and S2).  $27.9 \pm 6.0\%$  of all astrocytes were active in APP/PS1 mice when compared with the relatively rare spontaneous events seen in wild-type mice ( $8.1 \pm 2.3\%$ ;  $P < 0.05$ ) (Fig. 2B). APP/PS1 mutant mice did not show evidence of altered spontaneous activity before they developed senile plaques (at 3 to 3.5 months old) (Fig. 2B). Furthermore, the amplitude  $\Delta F/F$  of the calcium signals was significantly higher in APP/PS1 mice ( $\Delta F/F$ ,  $33.6 \pm 1.1\%$ ) when compared with that of wild-type mice ( $\Delta F/F$ ,  $23.2 \pm 0.8\%$ ,  $P < 0.001$ ) (fig. S4). This change in astrocytic function was also independent of plaque proximity (Fig. 2C and fig. S4), again implicating a global astrocytic response to plaque deposition. It was possible that our measurements of baseline resting calcium using FLIM (Fig. 1) reflected this increased astrocyte spontaneous activity rather than a change in baseline resting calcium. To test this, we coregistered FLIM data with spontaneous activity data to allow single-cell identification across imaging modalities. Spontaneously active cells did not have significantly different resting calcium than non-active cells (Fig. 1H,  $P = 0.811$ ).

In this mouse model, astrocytes do not produce A $\beta$ , which suggests a non-cell-autonomous mechanism behind the increased activity. Hyperactive neurons in the plaque penumbra (2) might be responsible by inducing increased activity in functionally connected astrocytes. To test this, we blocked neuronal activity with the sodium-channel blocker tetrodotoxin (TTX) (Fig. 2, D to F, and fig. S5). Under these conditions, astrocytic activity persisted (Fig. 2F). Thus, the increase in astrocyte activity does not derive from neuronal hyperactivity near A $\beta$  deposits, which supports the hypothesis that A $\beta$  interacts directly with the astrocyte network.

Astrocytes play a local role in supporting neuronal activity and in mirroring neuronal responses

<sup>1</sup>Massachusetts General Hospital, Department of Neurology/Alzheimer's Disease Research Laboratory, 114 16th Street, Charlestown, MA 02129, USA. <sup>2</sup>Program in Biophysics, Harvard University, Cambridge, MA 02138, USA.

\*To whom correspondence should be addressed. E-mail: bbacskai@partners.org